




Results of KVN Key Science Program for evolved stars

Youngjoo Yun¹, Se-Hyung Cho¹, Dong-Hwan Yoon¹, Haneul Yang¹,
Richard Dodson², María J. Rioja^{2,3} and Hiroshi Imai⁴

¹Korea Astronomy and Space Science Institute, 776 Daedeok-daero, Yuseong-gu, Daejeon 34055, Republic of Korea. email: yjyun@kasi.re.kr

²International Centre for Radio Astronomy Research, The University of Western Australia, 35 Stirling Highway, Western Australia, Australia

³Observatorio Astronómico Nacional (IGN), Alfonso XII, 3 y 5, E-28014 Madrid, Spain

⁴Center for General Education, Institute for Comprehensive Education, Kagoshima University 1-21-30 Korimoto, Kagoshima 890-0065, Japan

Abstract. We present the results of KVN Key Science Program (KSP) for evolved stars, which was launched in 2014. The first phase of KSP ended in June 2020 and the second phase started in October 2020. The goal of KSP is to study the physical characteristics of the evolved stars by observing the spatial distribution and temporal variability of the stellar masers at four frequency-bands (K, Q, W and D bands). The 22 GHz H₂O maser is usually observed from the outer part of circumstellar envelopes compared to the 43, 86, 129 GHz SiO masers, thus the kinematic links between these regions can be studied by the multi-frequency simultaneous observations of KSP along the stellar pulsation cycles. This eventually enable us to study the enormous mass-loss rate of evolved stars, and the accumulated results from KSP are expected to shed light on the study of the late stage of the stellar evolution.

Keywords. masers, radiative transfer, techniques: interferometric, stars: AGB and post-AGB, stars: circumstellar matter, stars: mass loss

1. Introduction

The SiO and H₂O masers are commonly observed from many oxygen-rich evolved stars and enable us to see the innermost part of circumstellar envelopes (CSEs) which consist of thick dust and gas layers ejected from the central stars. The masing conditions of the 22 GHz H₂O maser are usually fulfilled at the outer part of the CSEs compared to those of the 43, 86, and 129 GHz SiO masers (Richards *et al.* 2020). KVN can simultaneously observe the stellar masers at four frequency-bands, so the spatial distributions of individual masers can be directly compared each other in the KVN VLBI images. Therefore, the physical conditions as a function of the distance from the central stars can be estimated by KVN observations at once. Temporal variability of the intensities and the internal motions of the stellar masers can trace the movements of the gas and dust in the CSEs, which are closely related to the stellar pulsations (Höfner & Olofsson 2018). In order to study the mass-loss processes initiated in the inner part of the CSEs of evolved stars, the KVN Key Science Program (KSP) was launched in 2014. KSP monitoring observations toward the evolved stars have provided the dynamical characteristics of the stellar masers which enable us to trace the mass-loss processes and to study the origin of the morphological changes during the asymptotic giant branch (AGB) to the planetary nebula (PN). Many KSP data have shown the unprecedented results of the stellar masers, which have

been already published. Here we introduce some preliminary results, which are prepared for more comprehensive studies.

2. Source selection and observations

In the first phase of KSP (2014 - 2020), 16 sources were selected, from which the strong stellar masers were detected in preceding KVN single dish surveys. Seven sources have been observed in the second phase of KSP since 2020; 3 sources are newly added and the rest are overlapped with those of the first phase KSP. Most of the sources are oxygen-rich AGB stars and red supergiants except χ Cyg which is a S-type star.

The H₂O 6₁₆-5₂₃ (22.2 GHz) maser, the SiO $v=1, 2, J=1\rightarrow 0$ (43.1 GHz, 42.8 GHz) masers, and the SiO $v=1, J=2\rightarrow 1, J=3\rightarrow 2$ (86.2 GHz, 129.3 GHz) masers have been simultaneously observed toward the sources every month except the maintenance season (July and August). The receiving bandwidth is 256 MHz which consists of 16 base band channels (BBCs) yielding 1 Gbps recording rate. The velocity channel resolutions are 0.42, 0.22, 0.11, and 0.07 km s⁻¹ for K, Q, W, and D bands respectively, which are achieved by the Distributed FX (DiFX) software correlator (Deller *et al.* 2007).

Basic calibration of the observed data has been done using the Astronomical Image Processing System (AIPS), and further calibration such as the phase referencing process has been applied to the multi-band data using the source frequency phase referencing (SFPR) method (Dodson *et al.* 2014). The relative spatial distributions between the masers observed at four frequency-bands can be precisely determined by the SFPR method. Large amounts of the data accumulated from the long-term monitoring observations have been effectively reduced through the pipeline processes.

3. Preliminary results of several sources

Results of the first phase KSP have been published and also combined with those of the second phase for further comprehensive studies. The combined results cover the stellar pulsation period several times for most of the target sources so they enable us to trace the dynamical evolution of the CSEs affected by the pulsation-driven shock propagation. The spatial distributions of the masers are significantly different from source to source and also show the distinct temporal variability along the pulsation period of individual stars.

Figure 1 shows the contour maps of the masers observed at four frequencies toward VY CMa which is a supergiant showing locally-developed mass ejection (Decin *et al.* 2016). The spoke-like features (Zhang *et al.* 2012) of the SiO masers show the linearly-distributed density enhancement implying the mass loss along the radial direction. Therefore, the position of the central star can be determined by finding the intersection of the extended directions of individual spoke-like features. The north-east region is crowded with the SiO maser features in overall elliptical distribution, which implies the asymmetric motions in the inner part of the CSE. The asymmetric distributions of the SiO masers around VY CMa have been consistently observed during the KSP observations. The south-east part of the 22 GHz H₂O maser appears to be associated with the interface between the stellar wind and the large dense clump (Richards *et al.* 2014).

Figure 2 shows the typical ring-like structures of the SiO masers around IK Tau, the oxygen-rich Mira variable whose pulsation period is about 470 days (Hale *et al.* 1997). The left panel of Fig. 2 shows the results observed in January 2016 and the right panel shows the results observed in February 2020. The corresponding stellar phases are about 0.3 and 0.5 respectively. The circular distributions in January 2016 changed to the elliptical distributions in February 2020. The morphological changes of the SiO maser distributions from circle to ellipse or vice versa occur during the KSP monitoring observations. This might be related to the intrinsic anisotropy of the stellar pulsation

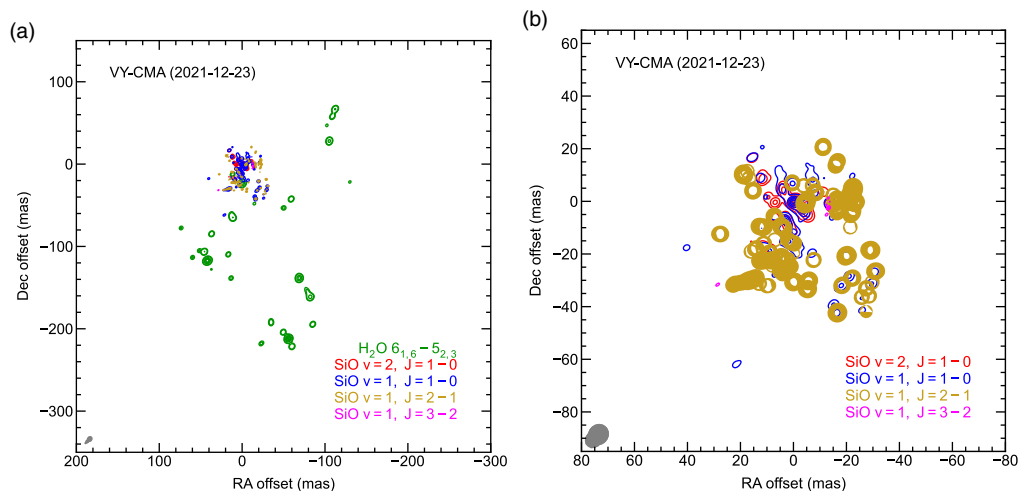


Figure 1. (a) Integrated intensity maps of the 22.2 GHz H₂O and 42.8/43.1/86.2/129.3 GHz SiO masers of VY CMA. (b) Enlarged plot of the SiO maser region.

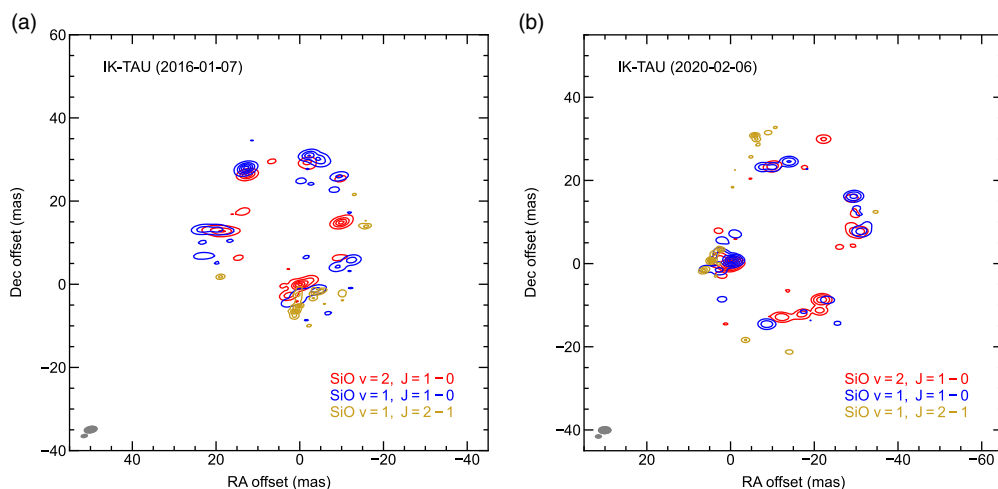


Figure 2. (a) Contour maps of 42.8/43.1/86.2 GHz SiO masers of IK Tau observed in January 2016. (b) Contour maps of 42.8/43.1/86.2 GHz SiO masers of IK Tau observed in February 2020.

and the high clumpiness of the CSE materials. Furthermore, the direction of the major axis of elliptical shape changed along the stellar pulsation, e.g., NE-SW direction in April 1996 (Boboltz & Diamond 2005) and NW-SE direction in February 2020 of KSP results. The relative spatial distributions between the different SiO masers around IK Tau show a somewhat consistent aspect, i.e., the $v=2, J=1 \rightarrow 0$ SiO maser occurs in innermost region and the $v=1, J=2 \rightarrow 1$ is detected in outermost region as shown in Fig. 2.

Figure 3 shows the velocity spot map of the $v=1, J=2 \rightarrow 1$ SiO maser around W Hya, the oxygen-rich AGB star. Its distance is about 100 pc (van Leeuwen 2007), and the mass-loss rate is in the range between 10^{-7} and $1.5 \times 10^{-7} M_{\odot} \text{ yr}^{-1}$ (Maercker *et al.* 2008; Khouri *et al.* 2014). Previous studies (Ohnaka *et al.* 2016; Khouri *et al.* 2020) found the strong visible and near-IR emissions from the clumpy dust envelopes in the north part. The $v=1, J=2 \rightarrow 1, J=3 \rightarrow 2$ SiO masers of W Hya show the bulging features in north and north-west parts of the ring-like structure in KSP observations. The north

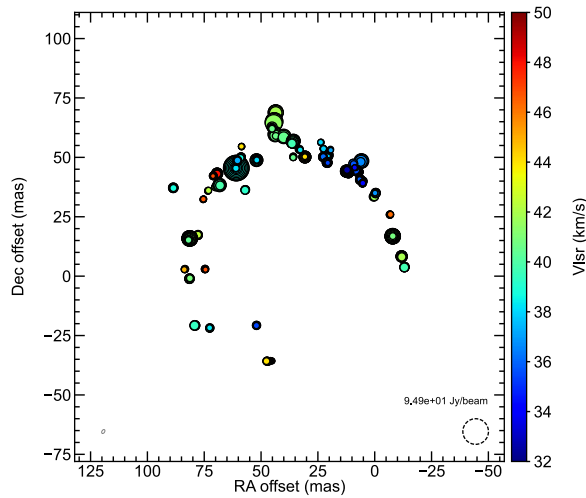


Figure 3. Velocity spot map of the $v=1$, $J=2\rightarrow 1$ (86.2 GHz) SiO maser emitted from the CSE of W Hya observed in December 2016. The stellar velocity is about 42 km s^{-1} . The maser intensities are represented by the circle areas varying with a logarithmic scale relative to the maximum flux density of $94.9 \text{ Jy beam}^{-1}$ indicated by a dotted circle at bottom-right corner.

clumpy structure lies at the stellar velocity of 42 km s^{-1} while the north-west bulge appears to be blue-shifted with respect to the stellar velocity. KSP observations have monitored the locally-enhanced mass ejection initiated in the inner part of the CSE of W Hya, which help us to study the mass-loss mechanism of AGB stars.

4. Summary

A large amount of data for the masers of evolved stars has been accumulated from the successful operation of KSP. The SFPR processes enable KSP to yield the astrometrically-registered maser images with a high accuracy up to sub-milliarcseconds (Dodson *et al.* 2014). The relative spatial distributions between the stellar masers have provided the crucial information to study the complicated physical environments of the CSEs of evolved stars. Furthermore, the results of long-term monitoring observations toward the stellar masers show the dynamical evolution of clumpy structures and the kinetic links between the inner part and the outer part of CSEs, thus they lead us to trace the mass-loss processes at the late stage of stellar evolution.

References

- Boboltz, D. A., & Diamond, P. J. 2005, *ApJ*, 625, 978
 Decin, L., Richards, A. M. S., Millar, T. J., *et al.* 2016, *A&A*, 592, A76
 Deller, A. T., Tingay, S. J., Bailes, M., & West, C. 2007, *PASP*, 119, 318
 Dodson, R., Rioja, M. J., Jung, T.-H., *et al.* 2014, *AJ*, 148, 97
 Hale, D. D. S., Bester, M., Danchi, W. C., *et al.* 1997, *ApJ*, 490, 407
 Höfner, S., & Olofsson, H. 2018, *A&AR*, 26, 1
 Khouri, T., de Koter, A., Decin, L., *et al.* 2014, *A&A*, 561, A5
 Khouri, T., Vlemmings, W. H. T., Paladini, C., *et al.* 2020, *A&A*, 635, A200
 Maercker, M., Schöier, F. L., Olofsson, H., Bergman, P., & Ramstedt, S. 2008, *A&A*, 479, 779
 Ohnaka, K., Weigelt, G., & Hofmann, K. H. 2016, *A&A*, 589, A9
 Richards, A. M. S., Impellizzeri, C. M. V., Humphreys, E. M., *et al.* 2014, *A&A*, 572, L9
 Richards, A. M. S., Sobolev, A., Baudry, A., *et al.* 2020, *AdSpR*, 65, 780
 van Leeuwen, F. 2007, *A&A*, 474, 653
 Zhang, B., Reid, M. J., Menten, K. M., & Zheng, X. W. 2012, *ApJ*, 744, 23